National Conference with International Participation

ENGINEERING MECHANICS 2008

Svratka, Czech Republic, May 12 – 15, 2008

2D MODEL OF A RIDER AND A POWERED TWO-WHEEL VEHICLE

P. Talaia*, M. Hajžman*

Summary: *The two dimensional (2D) model of a rider and a Powered Two-Wheeler (PTW) is proposed in this paper. The needs of such type of a model are summarized. The model is composed of rigid bodies connected by kinematic joints. The adopted modeling methodologies were the analysis in time domain using absolute Cartesian coordinates of the bodies. The model parameters, code implementation and simulation results are presented for a testing example. The results are discussed and conclusions are taken.*

1. Introduction

According with the European Commission, it was registered 50 000 casualties in the year of 2001 in the European roads (Tostmann, 2006). This number is decreasing slowly with the efforts of several entities, but the ratio of the casualties involving powered two-wheelers (PTWs) remains almost equal. The contribution of the PTWs is a total of 20 %.

In the PTW riding, the influence of the driver is important for the particular behavior of the system (Imaizumi et al., 1996). Usually, for the multi-body dynamical analysis of PTW simplified models of the rider, which using one or two bodies to represent all the upper parts of a human body (head, neck, thorax, abdomen, pelvis, upper and lower arms with hands), are employed. The difficulty to implement and control a more complex model of the human body with more degrees of freedom is the reason for the usage of the model consisting of one or two bodies. The aim of this paper is to develop a more complex model of a human rider and PTW intended for the simplified dynamical analysis and for the testing of control algorithms proposed in the next steps of the research.

The model will be useful for dynamical analysis of PTW accidents by simulating various pre-crash and crash scenarios and evaluation of the probability of rider's injuries.

2. Mathematical model

The development of the two dimensional rider and PTW model prepared according to the literature data can be divided into two main parts.

The human model was implemented using anthropometric data (Robbins, 1983), considering the lower segments of the body (legs) as a part of the PTW frame and the hands as a part of the handlebar. The five body model was used for the human body. It consists of a

* Eng. Pedro Talaia, MSc.; Ing. Michal Hajžman, Ph.D.: Department of Mechanics, Faculty of Applied Sciences, University of West Bohemia, Univerzitní 22, 306 14 Pilsen, Czech Republic; tel.: +420 377 632 330, fax: +420 377 632 302; e-mail: ptalaia@kme.zcu.cz, mhajzman@kme.zcu.cz

head, a neck, a body (thorax, abdomen and pelvis), an upper arm and a lower arm (see Fig. 1). The PTW model was implemented using the data from Suzuki GSX-R1000K1 (Sharp et al., 2004). The PTW was considered as the system of five bodies – a rear wheel, a front wheel, a swing arm, a main body (frame, handlebar, upper fork, hands, upper and lower legs, and foots), and a lower fork. The PTW was fixed to the ground in the rear wheel and the front wheel was constrained in the horizontal plane for a basic dynamical analysis. In the total, the assembly of the human body and the PTW is characterized by ten joints (nine revolute and one prismatic). The joints are actuated by passive force elements (spring-damper elements).

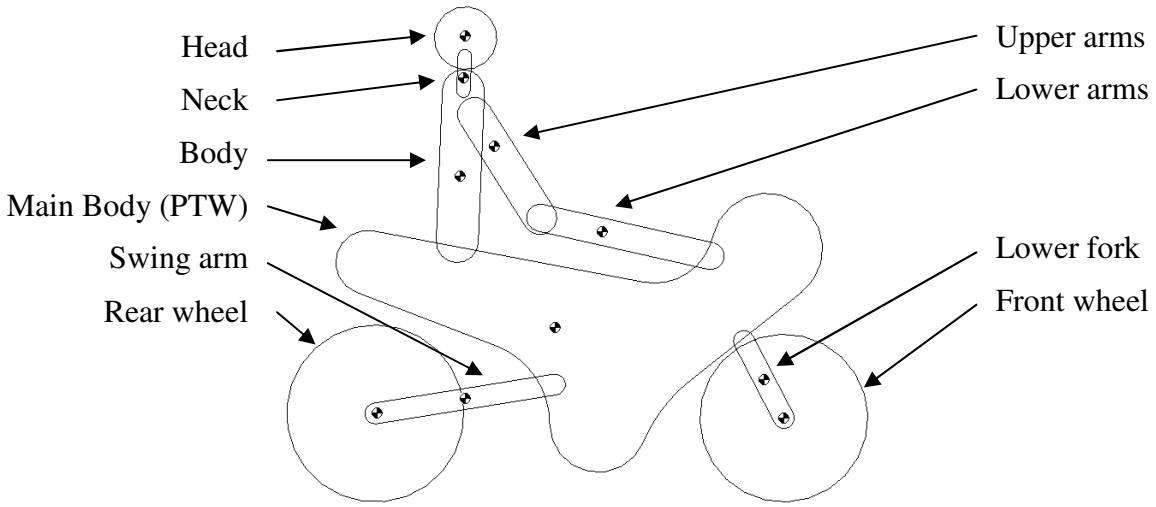

Fig. 1: Schematic representation of the Human body and PTW model (not to scale).

2.1. Theory background

Lagrange dynamics (Shabana, 2001) was used in order to form the mathematical model. Each body, performing planar motion, is described by three physical (Cartesian) coordinates. Two coordinates define the translation of the body center of mass, $\mathbf{R}^i = \begin{bmatrix} R_x^i & R_y^i \end{bmatrix}^T$, and the third defines the orientation of the body, θ.

The position vector of the arbitrary point of body i in the global inertia coordinate system can be expressed by

$$\mathbf{r}^i = \mathbf{R}^i + \mathbf{A}^i \cdot \bar{\mathbf{u}}^i, \tag{1}$$

where $\mathbf{A}^i$ is the transformation matrix due to the rotation of the local body reference frame and $\bar{\mathbf{u}}^i = \begin{bmatrix} u_x^i & u_y^i \end{bmatrix}^T$ is the local coordinates of the point in the body reference frame.

For each body we have generalized displacement vector $\mathbf{q}_i = \begin{bmatrix} R_x^i & R_y^i & \theta^i \end{bmatrix}^T$. The overall configuration space of the whole multibody system can be defined by the vector

$$\mathbf{q} = \begin{bmatrix} \mathbf{q}_1^T & \mathbf{q}_2^T & \mathbf{q}_3^T & \cdots & \mathbf{q}_n^T \end{bmatrix}^T. \tag{2}$$

To define the connection between the several bodies, we take a set of constrains. The constraint equations will be given by the vector $\mathbf{C}(\mathbf{q},t)$, composed of particular constraints

$$\mathbf{C}(\mathbf{q},t)=\left[\mathbf{C}_1(\mathbf{q},t)^T \quad \mathbf{C}_2(\mathbf{q},t)^T \quad \cdots \quad \mathbf{C}_{n_c}(\mathbf{q},t)^T\right]^T=0. \tag{3}$$

The Jacobian matrix in the form

$$\mathbf{C}_q=\begin{bmatrix} \frac{\partial \mathbf{C}_1}{\partial q_1} & \frac{\partial \mathbf{C}_1}{\partial q_2} & \frac{\partial \mathbf{C}_1}{\partial q_3} & \cdots & \frac{\partial \mathbf{C}_1}{\partial q_n} \\ \frac{\partial \mathbf{C}_2}{\partial q_1} & \frac{\partial \mathbf{C}_2}{\partial q_2} & \frac{\partial \mathbf{C}_2}{\partial q_3} & \cdots & \frac{\partial \mathbf{C}_2}{\partial q_n} \\ \vdots & \vdots & \vdots & \ddots & \vdots \\ \frac{\partial \mathbf{C}_{n_c}}{\partial q_1} & \frac{\partial \mathbf{C}_{n_c}}{\partial q_2} & \frac{\partial \mathbf{C}_{n_c}}{\partial q_3} & \cdots & \frac{\partial \mathbf{C}_{n_c}}{\partial q_n} \end{bmatrix} \tag{4}$$

plays the important role in the multibody system equations of motion derivation.

The mass matrix for a particular body can be described by equation

$$\mathbf{M}^i=\begin{bmatrix} m^i\,\mathbf{I} & \mathbf{0} \\ \mathbf{0} & J^i \end{bmatrix} \tag{5}$$

while for all bodies one can obtain

$$\mathbf{M}=\begin{bmatrix} \mathbf{M}^1 & & & & \\ & \mathbf{M}^2 & & 0 & \\ & & \ddots & & \\ & & & \mathbf{M}^i & \\ & 0 & & & \ddots \\ & & & & & \mathbf{M}^{n_b} \end{bmatrix}. \tag{6}$$

After applying Langrange's equations and several modifications, we get the system of differential-algebraic equations (e.g. Shabana, 2001) defined by

$$\begin{bmatrix} \mathbf{M} & \mathbf{C}_q^T \\ \mathbf{C}_q & \mathbf{0} \end{bmatrix}\cdot\begin{bmatrix} \ddot{\mathbf{q}} \\ \boldsymbol{\lambda} \end{bmatrix}=\begin{bmatrix} \mathbf{Q}_e \\ \mathbf{Q}_d \end{bmatrix}, \tag{7}$$

where $\mathbf{M}$ is the mass matrix, $\mathbf{C}_q$ is the Jacobian matrix of constraints, $\ddot{\mathbf{q}}$ is the acceleration vector, $\boldsymbol{\lambda}$ is the vector of Lagrange multipliers, $\mathbf{Q}_e$ is the vector of external forces, and $\mathbf{Q}_d$ is the vector that originates from the differentiation of the constraints, for our case given by equation

$$\mathbf{Q}_d=-\left(\mathbf{C}_q\cdot\dot{\mathbf{q}}\right)_q\cdot\dot{\mathbf{q}}. \tag{8}$$

In order to eliminate the Lagrange multipliers in the system (7), the equations can be modified and rewritten in the form

$$\boldsymbol{\lambda} = \mathbf{H}_{\lambda q} \cdot \mathbf{Q}_e + \mathbf{H}_{\lambda\lambda} \cdot \mathbf{Q}_d \,, \tag{9}$$

$$\ddot{\mathbf{q}} = \mathbf{M}^1 \cdot \mathbf{Q}_e + \mathbf{M}^{-1} \cdot \mathbf{C}_q^T \cdot \boldsymbol{\lambda} \,, \tag{10}$$

where the variables $\mathbf{H}_{\lambda\lambda}$, $\mathbf{H}_{qq}$ and $\mathbf{H}_{qq}$ are given respectively by

$$\mathbf{H}_{\lambda\lambda} = \left(\mathbf{C}_q \cdot \mathbf{M}^{-1} \cdot \mathbf{C}_q^T \right)^{-1}, \tag{11}$$

$$\mathbf{H}_{qq} = \mathbf{M}^1 + \mathbf{M}^{-1} \cdot \mathbf{C}_q^T \cdot \mathbf{H}_{\lambda\lambda} \cdot \mathbf{C}_q \cdot \mathbf{M}^{-1}, \tag{12}$$

$$\mathbf{H}_{q\lambda} = -\mathbf{H}_{\lambda q}^T = -\mathbf{M}^1 \cdot \mathbf{C}_q^T \cdot \mathbf{H}_{\lambda\lambda} \,. \tag{13}$$

2.2. Joint definition

To describe the rider and PTW multibody model, we have a total of nine (9) revolute joints and one prismatic joint. The joint passive actuators (springs and dampers) with the linear parameters obtained from the literature were introduced in order to represent suspension elements of the motorcycle and simplified physiological behavior of human joints.

2.2.1. Revolute joint

When two bodies are connected by a revolute joint, only relative rotation is allowed between both bodies. The figure 2 depicts two rigid bodies i and j that are connected by a revolute joint in the point P. It is clear from the figure that constraint points can be defined by absolute coordinates with respect to the global inertia coordinate system and thus the kinematic constraint conditions of the revolute joint can be stated by equation

$$\mathbf{R}^i + \mathbf{r}^i - \mathbf{R}^j - \mathbf{r}^j = \mathbf{0} \,. \tag{14}$$

A special case arises when one of the bodies is the ground. In this case we get the relation expressed by

$$\mathbf{R}^i + \mathbf{r}^i - \mathbf{c} = \mathbf{0} \,, \tag{15}$$

where **c** is the constant vector representing the position of the constraint point on the ground.

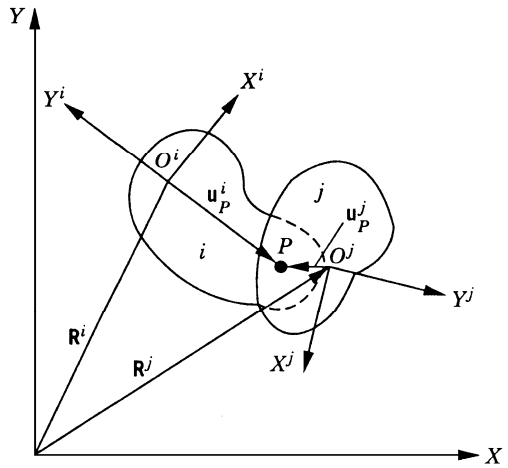

Fig. 2: Revolute joint (taken from Shabana, 2001).

2.2.2. Prismatic joint

A prismatic (translational) joint allows only relative translation between two bodies along the joint axis. Two degrees of freedom are constrained by this joint, defined by the respective equations. The definition of the constraint can be set by several ways. The adopted methodology is illustrated in Fig. 3.

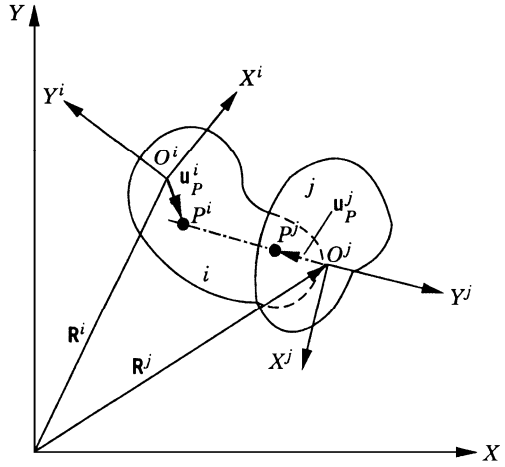

Fig. 3: Prismatic joint.

The adopted solution was the definition of the parallelism (no relative rotation) between two bodies

$$\theta^i - \theta^j - c = 0 \tag{16}$$

and the coincidence of the point P^i with the joint axis defined by the points P^j and O^j

$$\begin{cases} \mathbf{p}^1 = \mathbf{R}^i + \mathbf{A}^i \cdot \bar{\mathbf{u}}_p^i - \mathbf{R}^j - \mathbf{A}^i \cdot \bar{\mathbf{u}}_p^j \\ \mathbf{p}^2 = \mathbf{R}^i + \mathbf{A}^i \cdot \bar{\mathbf{u}}_p^i - \mathbf{R}^j \\ p_x^1 \cdot p_y^2 - p_y^1 \cdot p_x^2 = 0 \end{cases}, \tag{17}$$

since the translational axis in our case crosses the origin of the body reference frame.

2.3. Baumgarte's stabilization method

It is the fact that the constraint violation results from accumulated numerical integration errors and becomes more apparent with stiff systems (i.e. when natural frequencies of the system are widely spread). Even with the initial conditions not violating the constrains equations, during the course of numerical integration the numerical errors cause the violation of the constraint equations. The constant distance between two points can cease and the points move away from their initial position (Flores Fernandes, 2004; Hajžman & Polach, 2007).

When we are solving the equation (7), we are only satisfying the second derivative of the constraint equations. The solution can be improved by the replacement of the definition of the vector $\mathbf{Q}_d$ using expression

$$\mathbf{Q}_d = -\left(\mathbf{C}_q \cdot \dot{\mathbf{q}}\right)_q \cdot \dot{\mathbf{q}} - 2 \cdot \alpha \cdot \mathbf{C}_q \cdot \dot{\mathbf{q}} - \beta \cdot \mathbf{C}(\mathbf{q}, t) \tag{18}$$

The parameters α and β are arbitrary positive constants. It was not described the most optimal way how to choose these parameters in the literature. It depends on the nature of the solved problem and the suggestion of the parameters can be done by experimental tests.

3. Simulations, results and discussion

The described multibody model was implemented within MATLAB code (version 2007a). The numerical simulations were performed using the integration function *ode113* with a maximal step time of 2 ms, a relative error of 10^{-4} and an absolute error of 10^{-6}.

The initial positions and rotations of the centers of mass and inertial properties of the bodies are summarized in Tab. 1 and Tab. 2.

For visualization proposes, the user can see a list of various plots, and the animation of an entire simulation, displaying the PTW and the rider moving along the time.

Tab. 1: Initial position and rotation of the various centers of mass.

	Body number	$\overline{x}_P^i$	$\overline{y}_p^i$	θ^i
	-	$[m]$	$[m]$	$[°]$
Rear wheel	1	0.306	0.306	0.
Rear suspension	2	0.61523	0.36053	-0.1745
Front Wheel	3	1.82512	0.290	0
Fork	4	1.77382	0.43095	1.2217
Frame	5	1.01252	0.62296	0.
Trunk	6	0.91638	1.17101	1.7453
Lower arm	7	1.34786	1.21108	0.3263
Upper arm	8	1.10947	1.33741	0.5882
Neck	9	0.97523	1.50486	1.7453
Head	10	0.99887	1.63880	1.7453

Tab. 2: Mass and inertial moment of all bodies.

	Body number	m^i	J^i
	-	$[kg]$	$[\times 10^{-4}\ m]$
Rear wheel	1	15.500	5214.20
Rear suspension	2	10.000	2459.20
Front Wheel	3	20.000	7490.88
Fork	4	4.000	22.40
Frame	5	152.362	43361.57
Trunk	6	37.542	1011.218
Lower arm	7	4.044	61.850
Upper arm	8	3.538	24.206
Neck	9	0.965	24.206
Head	10	4.137	22.1552

3.1. Numerical example

Several simulations were performed to see the behavior of the model in several scenarios. In order to illustrate the capabilities following simulation were proposed: the first 3 seconds to observe the stabilization process (equilibrium) without any horizontal motion, then acceleration by 4 seconds followed by 3 seconds of stabilization, and 3 seconds of deceleration (80% front wheel and 20% rear wheel) and the following time to stabilization.

The system dynamic response for 20 seconds of simulation for the PTW frame, trunk and head is illustrated in Figs. 4 until 9 respectively. The initial and final position of the model is illustrated in Fig. 10. Horizontal direction is denoted by *xx* and vertical direction by *yy*.

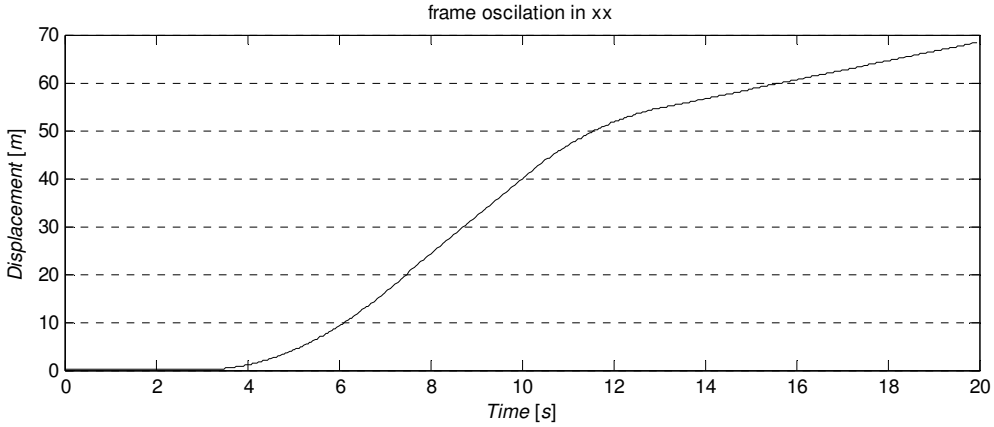

Fig.: 4: Frame oscillation in *xx* direction.

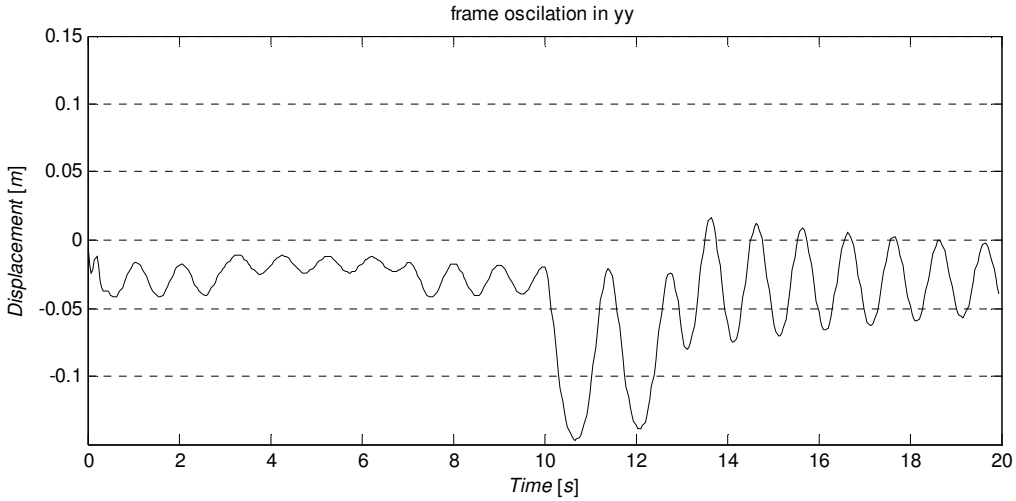

Fig.: 5: Frame oscillation in *yy* direction.

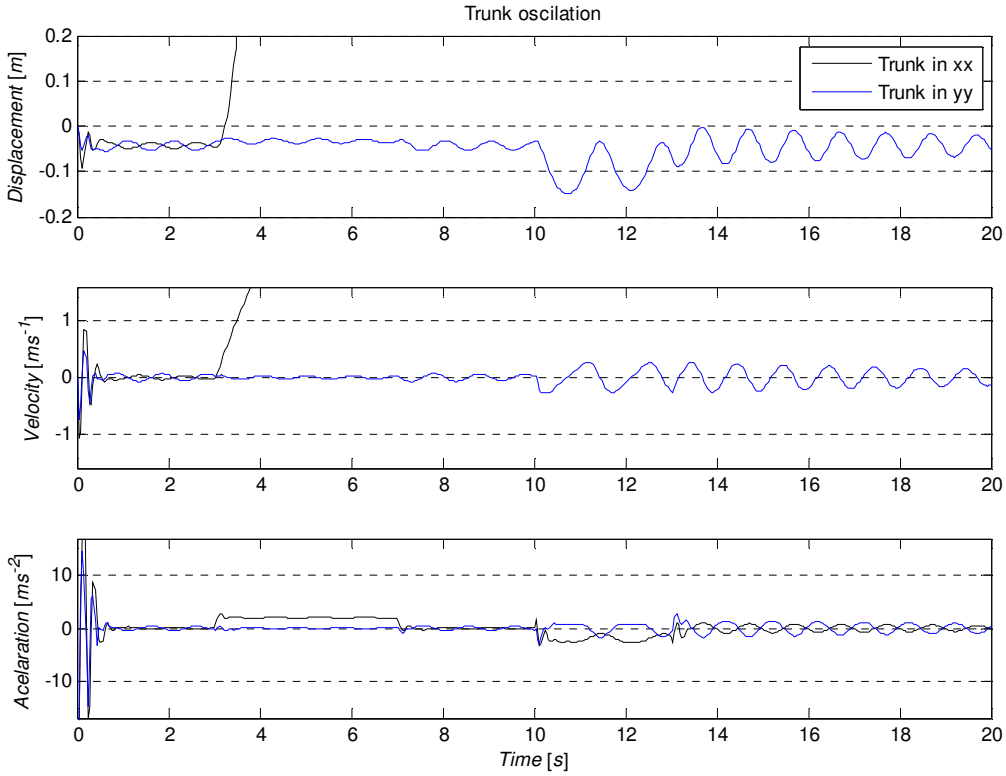

Fig. 6: Trunk oscillation (translational).

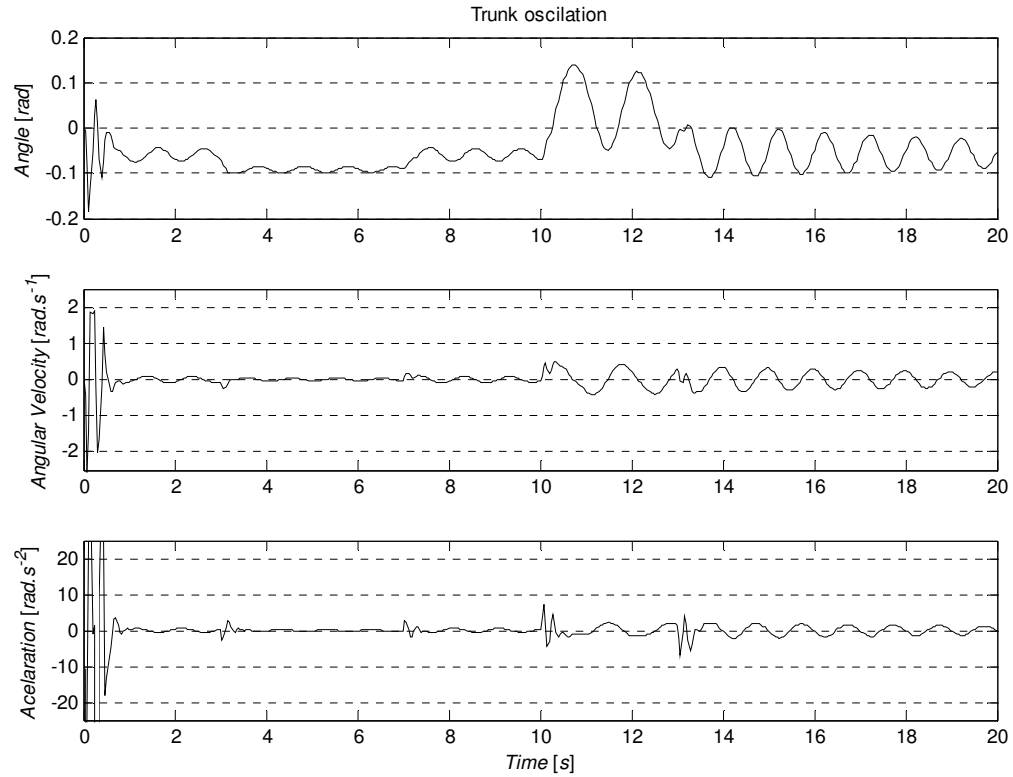

Fig. 7: Trunk oscillation (rotational).

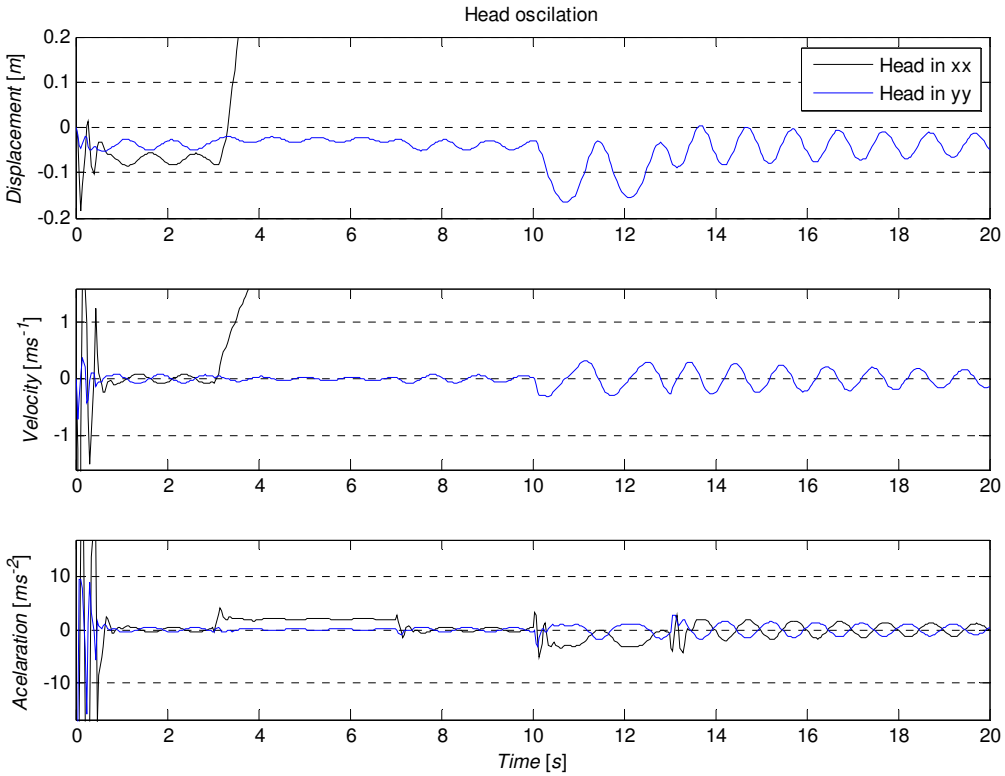

Fig. 8: Head oscillation (translational).

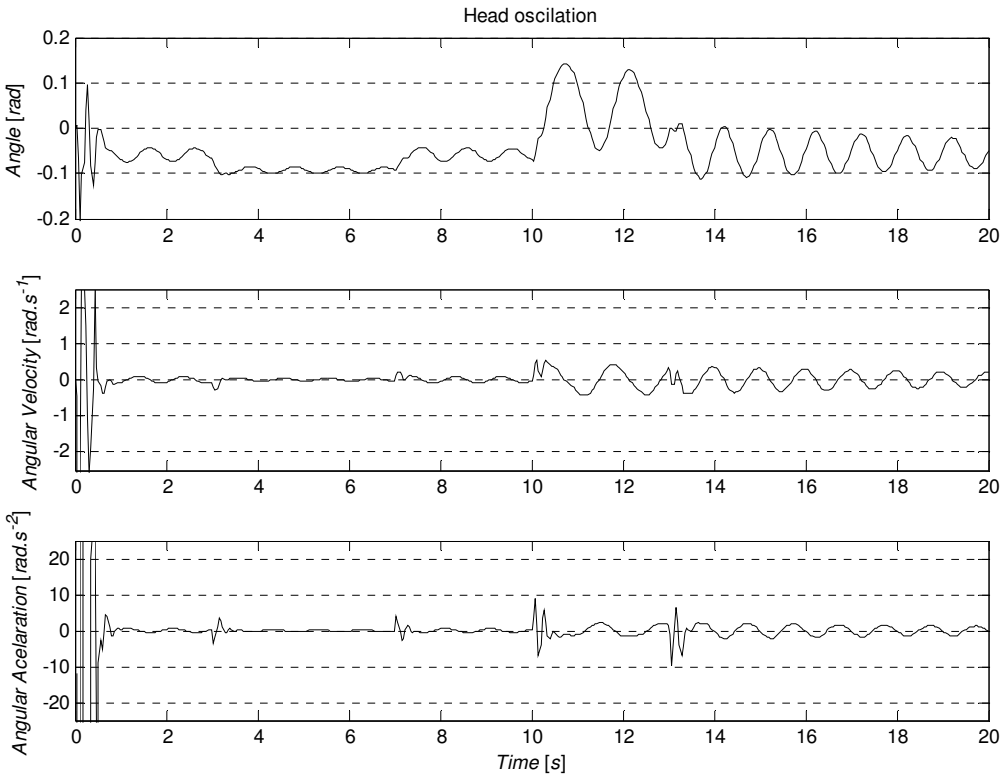

Fig. 9: Head oscillation (rotational).

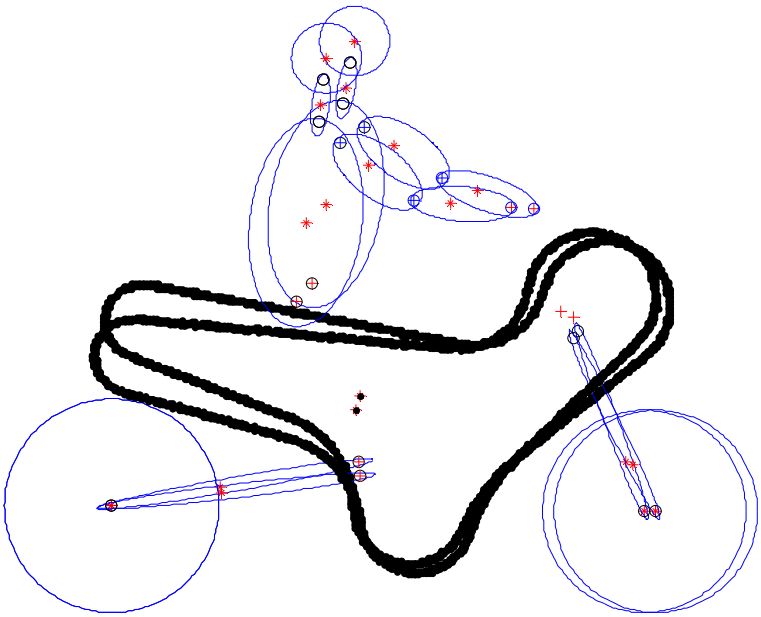

Fig. 10: Initial and final position of the model.

The simulation shows that for typical acceleration and deceleration values in the PTW the vibrations are relatively low. We can get in this stage the response of the system to several external excitations, which allow a better understanding of the system dynamics. These simulations will be improved with more complex joint definitions and compared with experimental data taken in volunteers in laboratory (pre-defined acceleration and brake maneuvers) and in real traffic environment.

The short movements of the head and the neck are obtained by the linearity of the used spring/damper and high stiffness in this anatomical position. The real values are for a relaxed articulation lower for this range of movements. The active joint wills stiffness too, but with a time delay by the answer time of the human body (reflex time). The used values were compromises between a passive model and a more realistic behavior. In this stage the value of damping was arbitrary, by the lack of information in the literature for this parameter.

Conclusions

The needs to understand the behavior of the human body in the position of a driver in a PTW is motivated by the investigation of some problems concerning accidents and by searching solutions for the safety improvement.

The presented work proposes the multi-body model that is able to analyze the planar motion of a rider and a PTW. The possibility to analyze acceleration, cruise and brake scenarios are possible, giving a better information of the human influence in the PTW behavior.

The fact that the 3rd axis is not presented is a limitation in the level of details, but advantage for the better control of the parameters in the given plane. Some of the planed

laboratory tests are taken in that plan with such type of scenarios (a constant acceleration or deceleration)

The need of experimental data in the present stage is a limitation for validation purposes. The tests in preparation will give the feed-back to validate and improve the model.

The change in the joint stiffnesses to more real curves must be followed by close-loop control too. This allows each human segment to move in a more realistic way.

The outputs of this model will help too in the parameterization of a 3D human body model, being implemented too in CAD/ CAE software.

Acknowledgement

The work is supported by the MYMOSA Marie Curie Actions project Nº MRTN-CT-2006-035965 of the European Community within the 6th Framework Program.

References

Hajžman, M & Polach, P. (2007) Application of stabilization techniques in the dynamic analysis of multibody systems. *Applied and Computational Mechanics*, 2, **1**, pp. 479-488

Imaizumi, H. et al. (1996) Rider model by use of multibody dynamics analysis. *JSAE*, 17, pp. 65-77.

Flores Fernandes, J. P. (2004) *Dynamic analysis of mechanical systems with imperfect kinematic joints*. PhD thesis, Escola de Engenharia, Universidade do Minho

Robbins, D. H. (1983) *Anthropometric specifications for mid-sized male dummy – Volume 2*. Michigan, University of Michigan.

Shabana, A. A. (2001) *Computational dynamics*, John Wiley & Sons, Inc.

Sharp, R. S. et al. (2004) Advances in the Modelling of Motorcycle Dynamics. *Multibody System Dynamics*, 12, pp. 251-283.

Tostmann, S. (2006) Powered two-wheelers and Road Safety: taking stock - looking ahead, in: *Proc. of Safety ACEM Conference*, Brussels.